K-Shell Core-Electron Excitations in Electronic Stopping of Protons in Water from First Principles

Yi Yao, Dillon C. Yost, and Yosuke Kanai

Phys. Rev. Lett. **123**, 066401 — Published 5 August 2019

DOI: 10.1103/PhysRevLett.123.066401

K-shell Core Electron Excitations in Electronic Stopping of Protons in Water from First Principles

Yi Yao, Dillon C. Yost, and Yosuke Kanai[*]

Department of Chemistry, University of North Carolina at Chapel Hill, North Carolina, 27599, USA

Understanding the role of core electron excitation in liquid water under proton irradiation has become important due to the growing use of proton beams in radiation oncology. Using a first-principles, non-equilibrium simulation approach based on real-time time-dependent density functional theory, we determine the electronic stopping power, the velocity-dependent energy transfer rate from irradiating ions to electrons. The electronic stopping power curve agrees quantitatively with experimental data over the velocity range available. At the same time, significant differences are observed between our first-principles result and commonly-used perturbation theoretic models. Excitations of the water molecules' oxygen core electrons are a crucial factor in determining the electronic stopping power curve beyond its maximum. The core electron contribution is responsible for as much as one-third of the stopping power at the high proton velocity of 8.0 a.u. (1.6 MeV). K-shell core electron excitations not only provide an additional channel for the energy transfer but they also significantly influence the valence electron excitations. In the excitation process, generated holes remain highly localized within a few angstroms around the irradiating proton path whereas electrons are excited away from the path. In spite of its great contribution to the stopping power, K-shell electrons play a rather minor role in terms of the excitation density; only 1% of the hole population comprises K-shell holes even at the high proton velocity of 8.0 a.u.. The excitation behavior revealed here is distinctly different from that of photon-based ionizing radiation such as X/γ-rays.

When a highly energetic ion travels through and interacts with matter, its kinetic energy is transferred into the target material's electronic and nuclear subsystems. This energy loss of the projectile ion can arise from both elastic collisions with nuclei (nuclear stopping) and inelastic scattering events (electronic stopping). When the particle's kinetic energy is sufficiently large (on the order of ~10 keV per nucleon), the major contribution to the energy transfer comprises electronic stopping wherein the projectile ion induces massive electronic excitations in the target matter[1-2]. This electronic stopping phenomenon is at the heart of emerging ion bean cancer therapies. The use of proton beam radiation over more conventional radiation based on X/γ-ray photons is often considered more effective because of the ion's distinct spatial energy deposition profile with a very sharp peak.[3-4] By calibrating the initial kinetic energy of the protons, this energy deposition peak can be tuned to coincide with the location of the tumour. This energy deposition profile is largely determined by electronic stopping power, which measures the rate of energy transfer from the charged particle to electrons in matter per unit distance of the energetic particle's movement.[1,5-7] The stopping power is a continuous function of the particle velocity, and the velocities near the maximum of the stopping power are responsible for the formation of the sharp energy deposition peak for ions like protons. Because liquid water makes up the majority of matter in human cells, various models have been developed for the electronic stopping power in liquid water over the years[8-16] including our earlier first-principles theory result[17-18]. At the same time, only limited experimental measurements exist near the stopping power maximum, and various theoretical models are currently used with empirically fitted parameters. Furthermore, unraveling the details of the excitation behavior in the electronic stopping process has become important. Proton radiation is generally considered as being similar to other types of ionizing radiation like X/γ-ray photons, which undergo Compton scattering and also core electron excitation. However, the extent to which proton radiation excites valence and core electrons is not understood. Indeed, this is complicated by the fact that the ratio of valence to core electron excitations depends on the irradiating proton velocity. In radiation oncology, an empirical factor such as relative biological effectiveness is used to take into account differences between the proton radiation and X-ray photon radiation for convenience, but many now call for a better mechanistic understanding of the radiation at the molecular level[19]. In this Letter, we discuss the role of K-shell core electron excitations in liquid water under proton irradiation by accurately determining the electronic stopping power and simulating

[*] E-mail: ykanai@unc.edu

quantum dynamics of electronic excitations from first principles.

We apply our recently developed non-equilibrium dynamics simulation approach based on real-time time-dependent density functional theory (RT-TDDFT)[17-18, 20-23] to simulate the non-perturbative response of the electronic system to a fast-moving projectile proton. In this approach, the electronic stopping power can be obtained from the rate of electronic energy change at different projectile proton velocities as discussed in our earlier work[21,24]. We use our implementation of RT-TDDFT based on a planewave-pseudopotential (PW-PP) formalism[20, 25] in the Qbox/Qb@ll code[26-27]. Simulating the 1s core (i.e. K-shell) electron excitations of oxygen atoms in this study requires us to go beyond several standard approximations typically used in the PW-PP formalism. The oxygen and hydrogen atoms in liquid water are described by all-electron pseudopotentials that are generated using the optimized Norm-Conserving Vanderbilt scheme[28-29], for which multiple projectors are used for the explicit treatment of the 1s electrons of oxygen atoms in the simulation. The validity of the all-electron pseudopotentials was checked by calculating the core-level optical excitation spectrum of a single water molecule as shown in the Supplemental Material. Unlike previous RT-TDDFT studies of electronic stopping in which pseudopotentials are used for the projectile proton[17-18], here we use a bare Coulomb potential for representing the proton because an accurate description of the K-shell core excitations is necessary, especially for large proton velocities (see Supplemental Material for details). Consequently, the use of a planewave kinetic energy cutoff of up to 250 Ry for expanding the Kohn-Sham wavefunctions was required, and an extrapolation was used for calculating the stopping power at high velocities (see Supplemental Material for details). We employed the PBE GGA approximation[30] for the exchange-correlation potential because we found that the use of the more advanced SCAN meta-GGA does not change the results[31-33] (Supplemental Material Fig. S7). The liquid water structure was generated by taking a snapshot after preforming a 10 ns classical molecular dynamics simulation at 300K with SPC/E force field[34]. Our simulation cell contains 38 water molecules with periodic boundary conditions (8Å × 8Å × 17.73Å), and the projectile proton travels in the +z direction. This simulation was compared to a larger simulation cell with 170 water molecules (12Å × 12Å × 35.45Å), and no appreciable finite size errors were found. In order to determine electronic stopping power accurately using the non-equilibrium simulation approach, an ensemble average of projectile proton trajectories is necessary[23]. 64 proton projectile trajectories (paths) were sampled evenly on a grid dividing the cross section of the xy simulation cell plane. In total, 64 independent RT-TDDFT simulations were performed for each velocity. The convergence of this sampling was confirmed by comparing to a more extensive sampling that includes 256 paths. Albeit computationally expensive, this trajectory sampling ensures that the ensemble average contains projectile proton trajectories that cover a wide range of impact parameters with respect to the atoms in the target matter, which is especially important when core electrons are excited[23,35]. The error bars on the stopping power reported here are the standard error of the mean calculated based on these 64 paths. Because the K-shell core electron excitation is found to be important in the high velocity regime, we also verified that close/small impact parameters are accurately sampled. These technical, but important, details are discussed in the Supplemental Material, in addition to comparisons to our earlier work[18], which did not consider core electron effects.

The calculated stopping power as a function of the proton velocity ranging from 0.5 to 8 a.u. (corresponding to the kinetic energy of 6.2 keV-1.6 MeV) is compared to the available experimental stopping power data[36-37] and to the so-called SRIM[16] model in Figure 1. The only experimental data available in this velocity range are the measurements by Shimizu, et al.[36-37]. We note, for completeness, that the reliability of this measurement has been questioned on the basis of the Bethe model[38]. The SRIM model is based on extending the Lindhard-Scharff-Schiott theory[39] with inputs from available experiments, and it is widely used as a standard reference. Though there is no reported experimental data for velocities less than 3.5 a.u. for liquid water, the SRIM result relies on existing experimental data of solid water (ice) to estimate the stopping power of liquid water. Our first-principles result is in excellent agreement with these two references. The peak of our calculated stopping power (i.e. the Bragg peak) is at v=1.73 a.u., and the stopping power of 0.165±0.010 a.u. agrees well with the SRIM model which shows the Bragg peak at v=1.72 a.u. and stopping power of 0.165 a.u. at this velocity. For comparison, we also show the seminal Bethe model[40] with mean excitation energy parameter of I=78eV as recommended by the International Commission on Radiation Units and Measurement[8] and one of the most recent models by Emfietzoglou and co-workers[10-12] based on perturbation theory. For the Bethe model, the Bragg peak lies around v=1.98 a.u. with a corresponding stopping power of 0.160 a.u.. As widely recognized, the Bethe model significantly underestimates the stopping power for low projectile velocities, and it does not obey the correct linear dependence around zero velocity[41]. At the same time, the Bethe model is remarkable in that the model correctly captures the stopping power behavior for the large projectile velocities beyond the peak velocity with only a single parameter to account for the target

matter, the mean excitation energy. The Emfietzoglou's model goes beyond the Bethe model, and it tends to the correct limits in both low and high velocities. However, Emfietzoglou's model shows the Bragg peak at around v=1.80 a.u. with the stopping power of 0.130 a.u., which significantly underestimates the magnitude of the electronic stopping power with respect to our first-principles result.

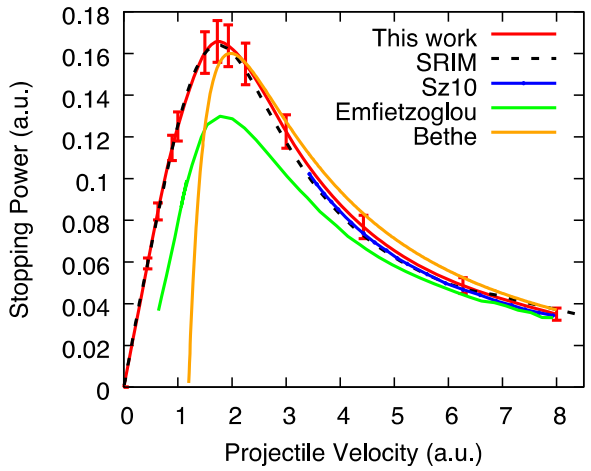

FIG 1 Electronic stopping power curve from our first-principles simulation, in comparison to the experimental data by Shimizu et al.[36-37] (Sz10), SRIM[16] model, the Bethe model[40] with I=78 eV recommended by International Commission on Radiation Units and Measurement[8], and the Emfietzoglou's model[10-12].

One of the most pressing challenges is to elucidate the importance of the K-shell core electron excitations. Widely used in radiation oncology, X/γ-ray radiation could effectively excite deep core electrons, undergoing Auger effect[42]. Empirical models have indicated that proton radiation does not excite K-shell core electrons appreciably for the proton velocities near the Bragg peak but only for much large velocities[11]. In recent years, differences between X/γ-ray and proton radiation have been examined more carefully in the radiation therapy literature[19]. However, our understanding of proton radiation is still quite limited, even for such an important biological matters like liquid water. Here, we examine the extent to which the K-shell core electron excitations play a role in the electronic stopping of protons in liquid water. In the literature, a separate K-shell contribution to stopping power is widely used, as in the Emfietzoglou's model[12]. However, in addition to providing an extra channel for the energy transfer from the projectile proton, electronic excitations of K-shell core electrons also influence the valence electron excitations. This is commonly known as "shake-up" effect[43] in the related context of X-ray absorption. In reality, it is therefore not possible to separate the electronic stopping power in terms of contributions from the valence electrons and core electrons independently as is widely done in empirical models[11-12,44-47]. Using first-principles theory, we can quantify how much the stopping power is influenced by the presence of the K-shell core electrons by calculating the stopping power with and without including the core electrons in our simulations as shown in the top panel of Figure 2. For convenience, we refer to the difference in these two stopping power curves as ΔS^{core}. The valence electron contribution indeed accounts for >99% of the stopping power for velocities less than 1.5 a.u. However, for the velocities larger than 1.5 a.u., the K-shell stopping power contribution, ΔS^{core}, starts to increase, from 0.002 a.u. (2% of the stopping power) at v=1.73 a.u. to 0.012 a.u. (25% of the stopping power) at v=6.27 a.u.. For the highest velocity of 8.0 a.u. we considered here, the stopping power is 28% higher when the core electrons are present. This observation differs significantly from the estimated K-shell electron contribution based on various empirical models (Emfietzoglou/Drude[11-12], and Hydrogenic generalized oscillator strength[11, 45, 48-49]) as shown in the bottom panel of Figure 2. For instance, the Emfietzoglou's model[12] predicts that the K-shell contribution starts to become important only at much greater velocities of > 3.5 a.u. (Figure 2 (Bottom)), and K-shell core electrons are responsible for less than 10% of the stopping power even at v=8.0 a.u..

* E-mail: ykanai@unc.edu

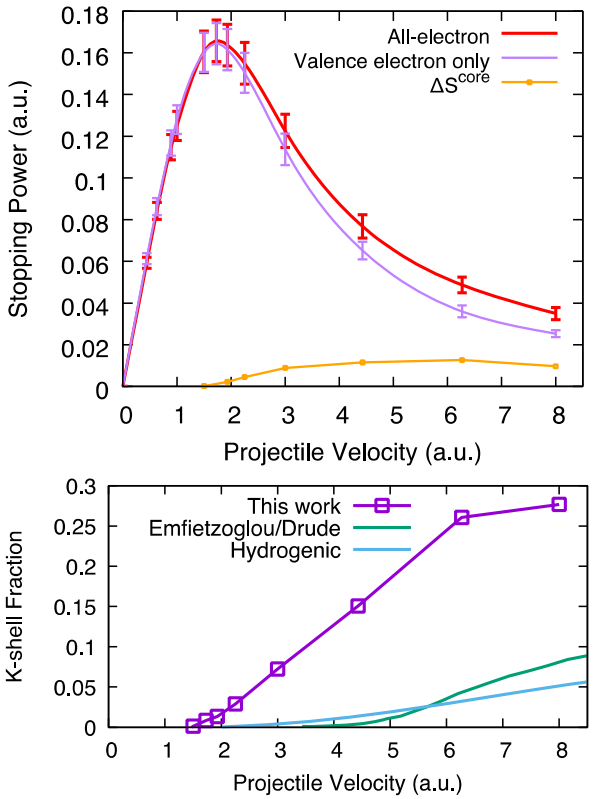

FIG 2 (Top) Contribution of the K-shell (oxygen 1s electrons) excitation to electronic stopping power curve, ΔS^{core}, calculated as the difference between the all-electron and the valence-electron only results. (Bottom) The fraction of the K-shell contribution to the stopping power, in comparison to the Emfietzoglou/Drude model[11-12], and Hydrogenic generalized oscillator strength model[11, 45, 48-49].

As discussed above, K-shell core electron excitations not only provide an extra channel for the energy transfer, but they also influence valence electron excitations. To quantify this shake-up effect in the electronic stopping, we calculated the summed expectation value of the Kohn-Sham (KS) Hamiltonian for all the valence electron wavefunctions, $\sum\langle\varphi_i(t)|\hat{H}_{KS}|\varphi_i(t)|\rangle$, in the simulations with and without the core electrons. The shake-up effect then can be quantified by obtaining the difference of this Hamiltonian expectation values for the valence electrons in the simulations with and without the K-shell core electrons. Figure 3 shows this energy difference as a function of the projectile proton displacement, averaged over all the 64 projectile paths. The shake-up effect contribution to the stopping power is obtained by calculating this expectation value change per unit distance of the projectile proton movement. At the high proton velocity of 8.0 a.u., the shake-up effect is responsible for 36 % of ΔS^{core} (i.e. 11 % of the stopping power). At the Bragg peak proton velocity of 1.73 a.u., 56 % of ΔS^{core} is due to the shake-up effect, but it is only <1% of the stopping power because K-shell core electrons are hardly excited at this peak velocity. For a very low velocity of 1.00 a.u., no shake-up effect is observed, and the difference between the all-electron and valence-electron-only calculations simply oscillates around zero in Figure 3. The K-shell core electron excitations have significant influence on the valence electron excitations at high velocities. Although having a separate correction for the core electron excitation is convenient in modeling[12, 23], it is not possible to take into account this intricate shake-up effect using such a model correction. This shake-up effect partly explains why using a separate K-shell correction underestimates the ΔS^{core} with respect to our first-principles result (see Figure 2 (bottom)).

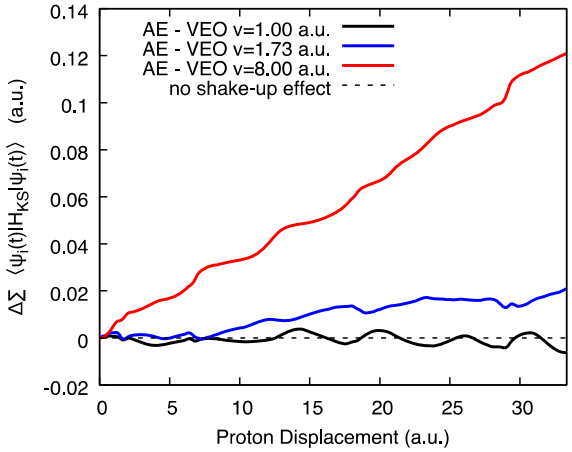

FIG 3 Difference of the summed Hamiltonian expectation value of the valence electrons for simulations with (all electrons - AE) and without K-shell core electrons (valence electron only - VEO) at the projectile proton velocity of 1.00 a.u., 1.73 (peak) and 8.00 a.u..

Having examined the K-shell core electron excitations and the importance of the shake-up effect, we now turn our attention to the spatial characteristics of the excited carriers in the electronic stopping process. The time-dependent Kohn-Sham (KS) wavefunctions can be projected onto the KS eigenstates of the equilibrium electrons to obtain the excited carrier distribution[17-18]. The projection onto the occupied and unoccupied eigenstates is used to calculate the hole and excited electron populations, respectively. All the occupied eigenstates and the unoccupied eigenstates up to 80 eV above the conduction band minimum are included in the projection, and the

electronic states covered in this energy range account for greater than 95% of the total excited electrons. At the peak velocity of v=1.73 a.u., the average number of holes per water molecule is 0.0933, and only 0.003% (3×10^{-6} holes) are generated in the K-shell. At v=8.0 a.u, the average number of holes is significantly smaller, 0.0108, but approximately 1% (1×10^{-4} holes) of the holes are generated in the K-shell. Figure 4 shows the spatial distribution of the excited electrons and holes at v=8.0 a.u., as a function of the distance from each projectile proton path, averaged over all the projectile paths. A full width at half maximum (FWHM) of the distribution for the core holes is 0.40 Å, while a noticeably broader FWHM of 2.38 Å is observed for the hole distribution in the valence band states. The valence hole distribution shows two notable features: a localized region that corresponds to individual water molecules along the path and the distribution tail that derives from neighboring water molecules. This tail component gives the valence hole distribution an appreciable magnitude even at distances larger than 5 Å. On the other hand, the excited electron distribution is not so localized along the projectile proton path as shown in Figure 4, and the excited electron distribution decreases only by ~10% even at 5 Å away from the path. This indicates that individual water molecules are indeed ionized along the projectile path in the electronic stopping process, consistent with our earlier finding[17] and also with the established notion of proton radiation as ionizing radiation. The K-shell core electron excitations still contribute greatly to the stopping power even when only a small proportion of the excited electrons are excited from the K-shell core states because the core excitation energy is a few orders of magnitude greater than the valence excitation energy.

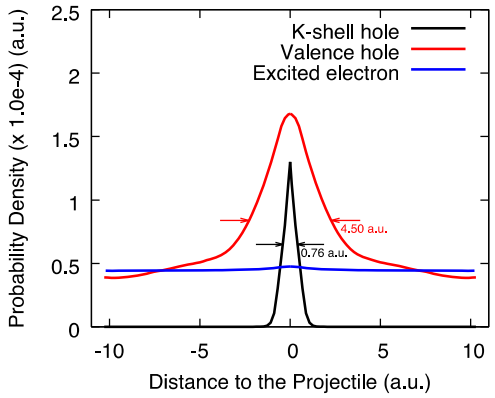

FIG 4 Ensemble-averaged distribution of holes and excited electrons as a function of the distance from the projectile proton path at the proton velocity of 8.0 a.u., the plot is made symmetric as a guide to the eye. The arrows indicate the FWHMs of the valence hole and O 1s hole distributions.

Developing a detailed understanding of the role of core electron excitations in liquid water under proton irradiation has become important largely due to the growing use of proton beams in radiation oncology. Using non-equilibrium simulations based on real-time time-dependent density functional theory, we accurately determined the electronic stopping power for protons in water from first principles, particularly focusing on the role of core electrons. The first-principles predicted stopping power shows significant differences to commonly-used perturbation theoretic models, such as the Bethe and Emfietzoglou models[12-13, 40]. The K-shell core electron excitation from water molecules' oxygen atoms was found to be crucial in determining the electronic stopping power curve beyond its maximum, being responsible for as much as one-third of the stopping power at the large proton velocity of 8.0 a.u. (the kinetic energy of 1.6 MeV). The core electron excitation significantly influences the valence electron excitation, in addition to providing an additional channel for the energy transfer. Such a cooperative phenomenon in the excitation is often refereed to as the shake-up effect[43], and this effect approximately accounts for as much as half of the contribution of the K-shell core electron excitation to the electronic stopping power at the high proton velocity of 8.0 a.u.. In the excitation process, the generated holes remain highly localized within a few angstroms around the irradiating proton path while electrons are excited away, indicative of ionizing radiation behavior. Despite their importance in contributing to the stopping power, the K-shell core electrons play a rather minor role in terms of the excitation density; only 1% of the holes is generated in the K-shell even at the large velocity of 8.0 a.u.. While X/γ-ray and proton radiations are both considered to be ionizing radiation and are usually treated on the same footing[19], our work revealed that the excitation/ionization behaviors involved are distinctly different.

ACKNOWLEDGMENT

The work is supported by the National Science Foundation under Grants No. CHE-1565714, No. DGE-1144081, and No. OAC-1740204. An award of computer time was provided by the Innovative and Novel Computational Impact on Theory and Experiment (INCITE) program. This research used resources of the Argonne Leadership Computing Facility, which is a DOE Office of Science User Facility supported under Contract DE-AC02–06CH11357.

REFERENCE

1. Race, C. P.; Mason, D. R.; Finnis, M. W.; Foulkes, W. M. C.; Horsfield, A. P.; Sutton, A. P., The treatment of electronic excitations in atomistic models of radiation damage in metals. *Reports on Progress in Physics* **2010,** *73* (11), 116501.

* E-mail: ykanai@unc.edu

2. Ziegler, J. F., Stopping of energetic light ions in elemental matter. *Journal of Applied Physics* **1999,** *85* (3), 1249-1272.
3. Scholz, M., Heavy ion tumour therapy. *Nucl Instrum Meth B* **2000,** *161*, 76-82.
4. Stelzer, H., Tumor therapy with heavy ions at GSI. *Nucl Phys B* **1998**, 650-657.
5. Kamaratos, E., The Mean Excitation-Energy for Stopping Power-I, the Bragg Rule, and Chemical and Phase Effects - Application of a Statistical Treatment to the Determination of I for Chemically Bound Particles. *Chem Rev* **1984,** *84* (6), 561-576.
6. Sigmund, P., *PARTICLE PENETRATION AND RADIATION EFFECTS: General Aspects and Stopping of Swift Point Charges* Springer: 2006; Vol. 151.
7. Sabin, J. R.; Oddershede, J.; Cabrera-Trujillo, R.; Sauer, S. P. A.; Deumens, E.; Öhrn, Y., Stopping power of molecules for fast ions. *Molecular Physics* **2010,** *108* (21-23), 2891-2897.
8. Report 90. *Journal of the International Commission on Radiation Units and Measurements* **2014,** *14* (1), 34-37.
9. Ashley, J. C., Optical-data model for the stopping power of condensed matter for protons and antiprotons. *Journal of Physics: Condensed Matter* **1991,** *3* (16), 2741.
10. Emfietzoglou, D.; Cucinotta, F. A.; Nikjoo, H., A Complete Dielectric Response Model for Liquid Water: A Solution of the Bethe Ridge Problem. *Radiation Research* **2005,** *164* (2), 202-211.
11. Emfietzoglou, D.; Garcia-Molina, R.; Kyriakou, I.; Abril, I.; Nikjoo, H., A dielectric response study of the electronic stopping power of liquid water for energetic protons and a new I-value for water. *Physics in Medicine & Biology* **2009,** *54* (11), 3451.
12. Emfietzoglou, D.; Nikjoo, H.; Pathak, A., Electronic cross sections for proton transport in liquid water based on optical-data models. *Nuclear Instruments and Methods in Physics Research Section B: Beam Interactions with Materials and Atoms* **2006,** *249* (1), 26-28.
13. Garcia-Molina, R.; Abril, I.; de Vera, P.; Kyriakou, I.; Emfietzoglou, D., A study of the energy deposition profile of proton beams in materials of hadron therapeutic interest. *Applied Radiation and Isotopes* **2014,** *83*, 109-114.
14. Penn, D. R., Electron mean-free-path calculations using a model dielectric function. *Physical Review B* **1987,** *35* (2), 482-486.
15. Ritchie, R. H., Energy losses by swift charged particles in the bulk and at the surface of condensed matter. *Nuclear Instruments and Methods in Physics Research* **1982,** *198* (1), 81-91.
16. Ziegler, J. F.; Ziegler, M. D.; Biersack, J. P., SRIM – The stopping and range of ions in matter (2010). *Nuclear Instruments and Methods in Physics Research Section B: Beam Interactions with Materials and Atoms* **2010,** *268* (11), 1818-1823.
17. Reeves, K. G.; Kanai, Y., Electronic Excitation Dynamics in Liquid Water under Proton Irradiation. *Scientific Reports* **2017,** *7*, 40379.
18. Reeves, K. G.; Yao, Y.; Kanai, Y., Electronic stopping power in liquid water for protons and alpha particles from first principles. *Physical Review B* **2016,** *94* (4), 041108.
19. Durante, M.; Orecchia, R.; Loeffler, J. S., Charged-particle therapy in cancer: clinical uses and future perspectives. *Nature Reviews Clinical Oncology* **2017,** *14*, 483.
20. Schleife, A.; Draeger, E. W.; Kanai, Y.; Correa, A. A., Plane-wave pseudopotential implementation of explicit integrators for time-dependent Kohn-Sham equations in large-scale simulations. *The Journal of Chemical Physics* **2012,** *137* (22), 22A546.
21. Schleife, A.; Kanai, Y.; Correa, A. A., Accurate atomistic first-principles calculations of electronic stopping. *Physical Review B* **2015,** *91* (1), 014306.
22. Yost, D. C.; Kanai, Y., Electronic stopping for protons and alpha particles from first-principles electron dynamics: The case of silicon carbide. *Physical Review B* **2016,** *94* (11), 115107.
23. Yost, D. C.; Yao, Y.; Kanai, Y., Examining real-time time-dependent density functional theory nonequilibrium simulations for the calculation of electronic stopping power. *Physical Review B* **2017,** *96* (11), 115134.
24. Pruneda, J. M.; Sánchez-Portal, D.; Arnau, A.; Juaristi, J. I.; Artacho, E., Electronic Stopping Power in LiF from First Principles. *Physical Review Letters* **2007,** *99* (23), 235501.
25. Schleife, A.; Draeger, E. W.; Anisimov, V. M.; Correa, A. A.; Kanai, Y., Quantum Dynamics Simulation of Electrons in Materials on High-Performance Computers. *Computing in Science & Engineering* **2014,** *16* (5), 54-60.
26. Gygi, F., Qbox open source code project. *Tech. Rep. (University of California, Davis)*.
27. Gygi, E. W. D. a. F., Qbox code, Qb@ll version. *Tech Rep. (Lawrence Livermore National Laboratory)*.
28. Hamann, D. R., Optimized norm-conserving Vanderbilt pseudopotentials. *Physical Review B* **2013,** *88* (8), 085117.
29. Schlipf, M.; Gygi, F., Optimization algorithm for the generation of ONCV pseudopotentials. *Computer Physics Communications* **2015,** *196*, 36-44.
30. Perdew, J. P.; Burke, K.; Ernzerhof, M., Generalized Gradient Approximation Made Simple. *Physical Review Letters* **1996,** *77* (18), 3865-3868.
31. Sun, J.; Remsing, R. C.; Zhang, Y.; Sun, Z.; Ruzsinszky, A.; Peng, H.; Yang, Z.; Paul, A.; Waghmare, U.; Wu, X.; Klein, M. L.; Perdew, J. P., Accurate first-principles structures and energies of diversely bonded systems from an efficient density functional. *Nature Chemistry* **2016,** *8*, 831.
32. Sun, J.; Ruzsinszky, A.; Perdew, J. P., Strongly Constrained and Appropriately Normed Semilocal Density Functional. *Physical Review Letters* **2015,** *115* (3), 036402.
33. Yao, Y.; Kanai, Y., Plane-wave pseudopotential implementation and performance of SCAN meta-GGA exchange-correlation functional for extended systems. *The Journal of Chemical Physics* **2017,** *146* (22), 224105.
34. Berendsen, H. J. C.; Grigera, J. R.; Straatsma, T. P., The missing term in effective pair potentials. *The Journal of Physical Chemistry* **1987,** *91* (24), 6269-6271.
35. Ullah, R.; Artacho, E.; Correa, A. A., Core Electrons in the Electronic Stopping of Heavy Ions. *Physical Review Letters* **2018,** *121* (11), 116401.
36. Shimizu, M.; Hayakawa, T.; Kaneda, M.; Tsuchida, H.; Itoh, A., Stopping cross-sections of liquid water for 0.3–2.0 MeV protons. *Vacuum* **2010,** *84* (8), 1002-1004.

37. Shimizu, M.; Kaneda, M.; Hayakawa, T.; Tsuchida, H.; Itoh, A., Stopping cross sections of liquid water for MeV energy protons. *Nuclear Instruments and Methods in Physics Research Section B: Beam Interactions with Materials and Atoms* **2009,** *267* (16), 2667-2670.
38. Garcia-Molina, R.; Abril, I.; de Vera, P.; Paul, H., Comments on recent measurements of the stopping power of liquid water. *Nuclear Instruments and Methods in Physics Research Section B: Beam Interactions with Materials and Atoms* **2013,** *299*, 51-53.
39. Lindhard, J.; Nielsen, V.; Scharff, M.; Thomsen, P., Integral equations governing radiation effects. *Mat. Fys. Medd. Dan. Vid. Selsk* **1963,** *33* (10), 1-42.
40. Bethe, H., Zur theorie des durchgangs schneller korpuskularstrahlen durch materie. *Annalen der Physik* **1930,** *397* (3), 325-400.
41. Ahlen, S. P., Theoretical and experimental aspects of the energy loss of relativistic heavily ionizing particles. *Reviews of Modern Physics* **1980,** *52* (1), 121-173.
42. Yokoya, A.; Ito, T., Photon-induced Auger effect in biological systems: A review. *International journal of radiation biology* **2017,** *93* (8), 743-756.
43. Persson, P.; Lunell, S.; Szöke, A.; Ziaja, B.; Hajdu, J., Shake-up and shake-off excitations with associated electron losses in X-ray studies of proteins. *Protein Science* **2001,** *10* (12), 2480-2484.
44. Garcia-Molina, R.; Abril, I.; Heredia-Avalos, S.; Kyriakou, I.; Emfietzoglou, D., A combined molecular dynamics and Monte Carlo simulation of the spatial distribution of energy deposition by proton beams in liquid water. *Physics in Medicine & Biology* **2011,** *56* (19), 6475.
45. Dingfelder, M.; Inokuti, M.; Paretzke, H. G., Inelastic-collision cross sections of liquid water for interactions of energetic protons. *Radiation physics and chemistry* **2000,** *59* (3), 255-275.
46. Date, H.; Sutherland, K.; Hayashi, T.; Matsuzaki, Y.; Kiyanagi, Y., Inelastic collision processes of low-energy protons in liquid water. *Radiation Physics and Chemistry* **2006,** *75* (2), 179-187.
47. Bernal, M.; Liendo, J., Inelastic-collision cross sections for the interactions of totally stripped H, He and C ions with liquid water. *Nuclear Instruments and Methods in Physics Research Section B: Beam Interactions with Materials and Atoms* **2007,** *262* (1), 1-6.
48. Heredia-Avalos, S.; Garcia-Molina, R.; Fernández-Varea, J. M.; Abril, I., Calculated energy loss of swift He, Li, B, and N ions in Si O 2, Al 2 O 3, and Zr O 2. *Physical Review A* **2005,** *72* (5), 052902.
49. Garcia-Molina, R.; Abril, I.; Denton, C. D.; Heredia-Avalos, S.; Kyriakou, I.; Emfietzoglou, D., Calculated depth-dose distributions for H+ and He+ beams in liquid water. *Nuclear Instruments and Methods in Physics Research Section B: Beam Interactions with Materials and Atoms* **2009,** *267* (16), 2647-2652.
50. See Supplemental Material [url] for computational details and comparison to earlier RT-TDDFT result and empirical/analytical models, which includes refs. [51-53].
51. Nilsson, A.; Nordlund, D.; Waluyo, I.; Huang, N.; Ogasawara, H.; Kaya, S.; Bergmann, U.; Näslund, L. Å.; Öström, H.; Wernet, P.; Andersson, K. J.; Schiros, T.; Pettersson, L. G. M., X-ray absorption spectroscopy and X-ray Raman scattering of water and ice; an experimental view. *Journal of Electron Spectroscopy and Related Phenomena* **2010,** *177* (2), 99-129.
52. Fonseca Guerra, C.; Handgraaf, J. W.; Baerends, E. J.; Bickelhaupt, F. M., Voronoi deformation density (VDD) charges: Assessment of the Mulliken, Bader, Hirshfeld, Weinhold, and VDD methods for charge analysis. *Journal of computational chemistry* **2004,** *25* (2), 189-210.
53. Schiwietz, G.; Grande, P., Improved charge-state formulas. *Nuclear Instruments and Methods in Physics Research Section B: Beam Interactions with Materials and Atoms* **2001,** *175*, 125-131.

* E-mail: ykanai@unc.edu